

## Electrodeposition of Ternary Zn-Cr<sub>2</sub>O<sub>3</sub>-SiO<sub>2</sub> Nanocomposite Coating on Mild Steel for Extended Applications

N. Malatji\*, A.P.I. Popoola\*

Department of Chemical, Metallurgical and Materials Engineering, Tshwane University of Technology, Pretoria, South Africa.

\*E-mail: [doublen.malatji@gmail.com](mailto:doublen.malatji@gmail.com); [malatjin@tut.ac.za](mailto:malatjin@tut.ac.za); [popoolaapi@tut.ac.za](mailto:popoolaapi@tut.ac.za)

*Received:* 12 August 2014 / *Accepted:* 11 February 2015 / *Published:* 23 March 2015

---

Nano-materials surface engineering is the key constituent for advanced manufacturing and high performance engineering components. Zn-Cr<sub>2</sub>O<sub>3</sub>-SiO<sub>2</sub> nanocomposite coatings were produced from electrolytic chloride bath solution on the surface of mild steel. The surface morphology, structural analysis and composition of the coatings was studied using Scanning electron microscope equipped with energy dispersive spectrometry (EDS) and X-ray diffractometer. The mixed oxide nanocomposite incorporated coating revealed a modification in crystallographic orientation and refinement of crystals was observed. Potentiodynamic polarization technique was used to investigate the corrosion behavior of the composites in 3.65% NaCl solution. The nanocomposites were also evaluated for their mechanical and tribological properties using CETR reciprocating sliding tester and diamond base microhardness indenter respectively. Zn-2.5g/L Cr<sub>2</sub>O<sub>3</sub>-7.5g/L SiO<sub>2</sub> exhibited better corrosion resistance and high microhardness values. An improvement in tribological behavior was also achieved for all the composites coatings fabricated. Heat treatment tests showed that the composite coatings exhibit better thermal stability properties than Zn coatings.

---

**Keywords:** Zn, Ternary Zn-Cr<sub>2</sub>O<sub>3</sub>-SiO<sub>2</sub> Nanocomposite Coating, Microhardness, Corrosion, Heat treatment and Tribology

### 1. INTRODUCTION

Surface engineering entails modifying the microstructure of the metallic surface matrix in order to impact functional properties that have the capabilities of decreasing the degradation and extending lifespan over time. This is accomplished by making the surface tough to the environment in which it will be used. In the past few years, nanotechnology has found its application in fabrication of metal coatings for enhancement of surface protection. Their ease of incorporation, uniform dispersion

attained and the excellent properties transferred into metal matrixes have increased the interest of researchers. They exhibit unusual properties that are not possessed in the traditional bulk material of the same kind [1]. It has been reported by many researchers that the incorporation of these nanocomposite materials into traditional coatings can improve the corrosion resistance, thermal stability, wear resistance, self-lubrication, mechanical and bio-compatibility properties [2-7].

Electrodeposition is one of the techniques that is used for the fabrication of nanocomposite coatings. This owes to several advantages that this technique possesses over other deposition techniques. These include easy control and homogeneity in deposition of complex shapes, reduced contamination, easily available equipment, high production rates, low costs and easily transferable from research lab to industrial scale [8-9]. The development of zinc matrix to improve the surface properties of the coatings, counter act the formation of white rust and meet demanding and increasing industrial applications which have led to exploration of new materials. These include the incorporation of nickel, copper, alumina, titania, silica, zirconia, silicon carbide etc., to produce zinc alloy/nanocomposite coatings [10-15].

Metal oxide nanoparticles are widely used for the fabrication of composites due to their availability. Srivastava et al studied electrodeposition of nickel with  $\text{Cr}_2\text{O}_3$  nanoparticles in a sulphamate bath and found that the incorporation of these nanoparticles have no effect on the corrosion resistance of brass, but improved tribological and mechanical properties [11]. The knowledge of fabrication of Zn- $\text{Cr}_2\text{O}_3$  composite coatings is scanty in literature.

Several authors have successfully codeposited Zn with  $\text{SiO}_2$  to fabricate Zn- $\text{SiO}_2$  composite coatings. Kundo et al reported  $\text{SiO}_2$  particles to refine the crystal grains and precipitate on the Zn hexagonal crystal plane when they were incorporated into Zn matrix using electrodeposition process [21]. The incorporation of  $\text{SiO}_2$  particles into a Zn matrix were also found to be dependent on bath composition and parameters [22]. The co-deposition of nano- $\text{SiO}_2$  into Zn-Ni matrix was found to improve the surface properties such as microhardness, corrosion resistance, wear resistance and thermal stability [9]. However, the thermal and tribological properties of the coatings have not been thoroughly investigated.

Work on the incorporation of nano- $\text{Cr}_2\text{O}_3$  into a Zn matrix to improve the properties of the coatings is scanty. No report has been published on the synergetic effect of nano- $\text{Cr}_2\text{O}_3$  and  $\text{SiO}_2$  particles inclusion in a Zn matrix.  $\text{Cr}_2\text{O}_3$  particles exhibit excellent thermal protection, wear and friction characteristics [23]. Particles of  $\text{SiO}_2$  have been reported to possess good chemical, mechanical and insulating properties [9]. Therefore, this research seeks to investigate the synergetic effect of  $\text{Cr}_2\text{O}_3$  and  $\text{SiO}_2$  nanoparticles in electrodeposited Zn matrix. The morphological, electrochemical, tribological and thermal characteristics of the nanocomposite coatings are been studied in this work.

## 2. EXPERIMENTAL METHODS AND MATERIALS

### 2.1. Sample Preparation

Zn and Zn- $\text{Cr}_2\text{O}_3$ - $\text{SiO}_2$  nanocomposite coatings were prepared by electrodeposition technique using mild steel plates as cathodes. The mild steel plates were sectioned using a cutting wheel to

dimensions of 25x40 mm. Emery papers of grit size of 180 and 400 grits were used to grind, polish and remove the unwanted materials such as rust on the mild steel substrate. The polished samples were then dipped into ethanol to remove the grease or oil on the mild steel followed by suspension into 1M HCl to activate the surface prior to plating. The plating solutions were mechanically stirred using a magnetic stirrer for 18 hours to keep Cr<sub>2</sub>O<sub>3</sub> (100 nm) and Al<sub>2</sub>O<sub>3</sub> (50 nm) nanoparticles in suspension.

**Table 1.** Bath Composition and Operating Conditions

Composition	Parameters
ZnCl <sub>2</sub> – 150 g/ L	Cathode – Mild steel
KCl – 50 g/L	Anode – Zn
Boric Acid – 30 g/L	Temperature – 25 °C
Glycine – 30 g/L	pH – 3.8
Thioarea – 10 g/L	Current – 1.5A
Cr <sub>2</sub> O <sub>3</sub> – 2.5, 5, 7.5 g/L	
SiO <sub>2</sub> – 2.5, 5, 7.5 g/L	

During electrodeposition, two Zn plates were used as anodes and the pH was kept constant at 3.8. The deposition time for the experiments was 20 minutes under ambient conditions while stirring at a speed of 300 rpm. The samples were rinsed in water for 5 seconds to remove loosely adhered particles and air dried after electrodeposition. Sample codes and description are as follows: [ZC1 = Zn-10g/L Cr<sub>2</sub>O<sub>3</sub>, ZC2 = Zn-20g/L Cr<sub>2</sub>O<sub>3</sub>, ZS1 = Zn-5g/L SiO<sub>2</sub>, ZS2 = Zn-10g/L SiO<sub>2</sub>, ZCS1 = Zn-2.5g/L Cr<sub>2</sub>O<sub>3</sub>-7.5g/L SiO<sub>2</sub>, ZCS2 = Zn-5g/L Cr<sub>2</sub>O<sub>3</sub>-5g/L SiO<sub>2</sub> and ZCS3 = Zn-7.5g/L Cr<sub>2</sub>O<sub>3</sub>-2.5g/L SiO<sub>2</sub>]

## 2.2 Surface characterization

JEOL-JSM-5800V scanning electron Microscope was used to study the morphological characteristics of the as-received mild steel sample, powders and electrodeposited samples. The compositional analysis of the samples were done using Energy Dispersive Spectrometry (EDS) affixed to the microscope. The structural analysis of the coatings was conducted using PANalytical X'Pert Pro diffractometer.

## 2.3 Microhardness testing

Diamond indenter microhardness tester was used to investigate the microhardness properties of the samples. The values reported are an average of three indentation measurements made at different locations.

## 2.4 Electrochemical behavior

Electrochemical measurements were performed using  $\mu$ AUTOLAB Pontentiostat/Galvanostat to investigate the corrosion properties of the samples in 3.65% NaCl environment. The polarization

measurements were carried from a start potential of -1.5 to end potential 1.5V at a scanning rate of 0.001V/s. Saturated calomel electrode was used as a reference and graphite rod as counter electrode were employed for the measurements in a conventional three electrode electrochemical cell. All the tests were conducted under ambient conditions with specimen of area 1 cm<sup>2</sup> was exposed to 3.65% solution.

### 2.5 Thermal stability

The coatings were subjected to annealing temperature of 250 °C in a laboratory tube furnace to study their thermal stability. The samples were exposed to heat treatment conditions for a time range of 0.5, 2 and 16 hours to study their thermal stability with respect to time for industrial applications where they are required to perform under high temperatures.

### 2.7 Wear

For wear performance studies, the samples were evaluated using CETR tribo-tester under dry reciprocating conditions. The coefficient of friction was continually recorded for a duration of 1000 seconds. All the tests were conducted at a constant normal load of 5N, sliding velocity of 2 m/s and sliding distance of 2 mm. The micrographs of the worn out surfaces were observed using Scanning electron microscope (100X). Dry abrasion rig machine was used to determine the percentage wear mass loss under dry sliding conditions using silica sand as a wearing medium at a speed of 200 rev/min for 60 sec. The initial mass of the samples were weighed before the tests and the final masses were recorded after the dry sliding. These values were used to determine the percentage wear mass loss.

## 3. RESULTS AND DISCUSSION

### 3.1. Characterization of As received sample and powders

The SEM micrographs of as received substrate, Cr<sub>2</sub>O<sub>3</sub> and SiO<sub>2</sub> nanopowders are shown in Fig. 1 below. Fig. 1 (a) shows as received sample which possesses a porous surface. These pores may serve as the degradation initiation sites where the material can be exposed to oxidative and corrosive environments. Cr<sub>2</sub>O<sub>3</sub> nano-powder as depicted by Fig. 1 (b) shows ununiform and agglomerated distributed particles. This result suggests that the particles requires intense agitation to keep them in suspension in solution to promote uniform incorporation in the metal matrix during electrodeposition. On the other hand, SiO<sub>2</sub> powder shows fine and uniformly distributed particles as depicted by Fig. 1 (c). The particle orientation of SiO<sub>2</sub> suggest that the particles can be easily embended in the Zn matrix to fill the pores and microholes, and hence improve the surface properties of these coatings.

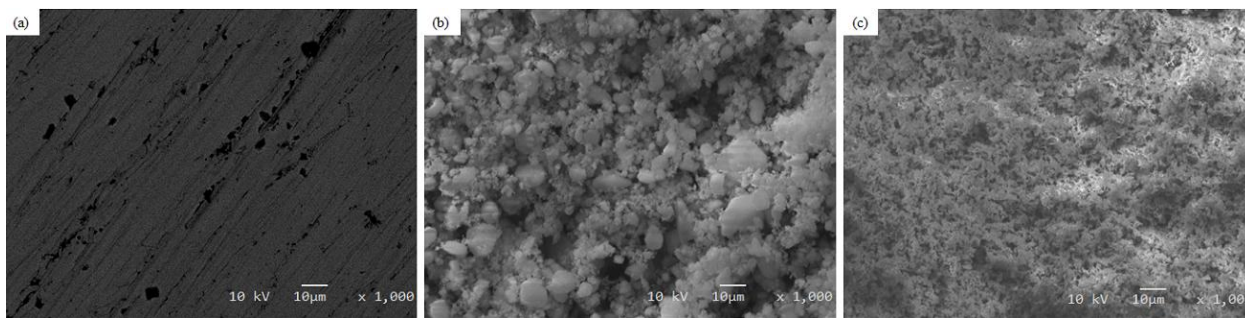


**Figure 1.** SEM micrographs for the received materials (a) Mild steel, (b) Cr<sub>2</sub>O<sub>3</sub> powder and (c) SiO<sub>2</sub> powder.

3.2. Effect of bath particle loading on microhardness

The microhardness values of the as received, zinc and composite coatings are presented in Fig. 2. An improvement in microhardness can be observed for all the composite samples compared with the as received sample and Zn coating. An increase in Cr<sub>2</sub>O<sub>3</sub> particle concentration in the bath for ZC composite samples resulted in improvement of microhardness of the Zn matrix. The microhardness increased from 161 to 228HVN at 10 and 20g/L Cr<sub>2</sub>O<sub>3</sub> particle loading in the bath respectively. This improvement can be attributed to the increment of Cr<sub>2</sub>O<sub>3</sub> nanoparticulates in solution which promotes the availability of the particles at the cathode to be embedded in the Zn matrix leading to more incorporation of the nanoparticles. Guglielmi ‘s two step adsorption model [17] support the result that was obtained for ZC1 and ZC2. However for ZS samples, no increase in microhardness was found when SiO<sub>2</sub> particle content was increased from 5 to 10 g/L . Agglomeration of particles in the bath which can caused by exceeding optimal particle concentration may be the cause of no further improvement in microhardness yield of the composite. Agglomeration of particles in the plating bath reduce the availability of the particles at the cathode and thus hinder their uniform incorporation into the Zn matrix as explained by [3].

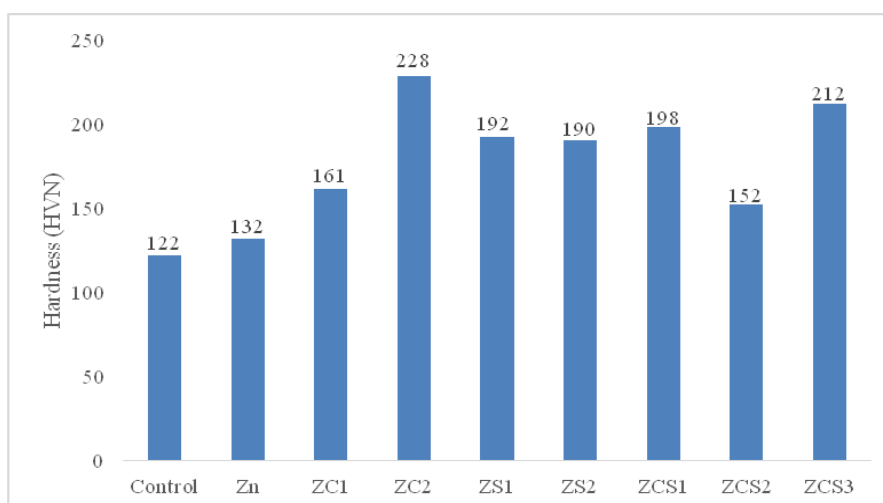


**Figure 2.** Microhardness values for as received, Zn, binary and ternary composite coatings

It can be observed from the ZCS samples that increment in the bath content of Cr<sub>2</sub>O<sub>3</sub> nanoparticulates resulted in the highest microhardness yield in ZCS3. Therefore, it can be concluded that the optimal concentration of the particles in the plating bath for improved microhardness yield for ZCS nanocomposite coatings is 7.5 Cr<sub>2</sub>O<sub>3</sub> and 2.5g/L SiO<sub>2</sub>. These results showed that incorporation of Cr<sub>2</sub>O<sub>3</sub> and SiO<sub>2</sub> nanoparticles have positive synergetic effect on the mechanical properties of Zn matrix.

### 3.3 Electrochemical Behavior

The electrochemical tests were conducted using linear polarization in 3.65% NaCl solution. The polarization curves of as received, Zn and nanocomposites samples has been plotted and are shown in Fig. 3. The corrosion parameters such as corrosion potential ( $E_{\text{corr}}$ ), corrosion current density ( $I_{\text{corr}}$ ) and anodic and cathodic Tafel slopes ( $\beta_a$  and  $\beta_c$ ) are presented in Table 2. The corresponding corrosion reactions are as follows:

Anodic process

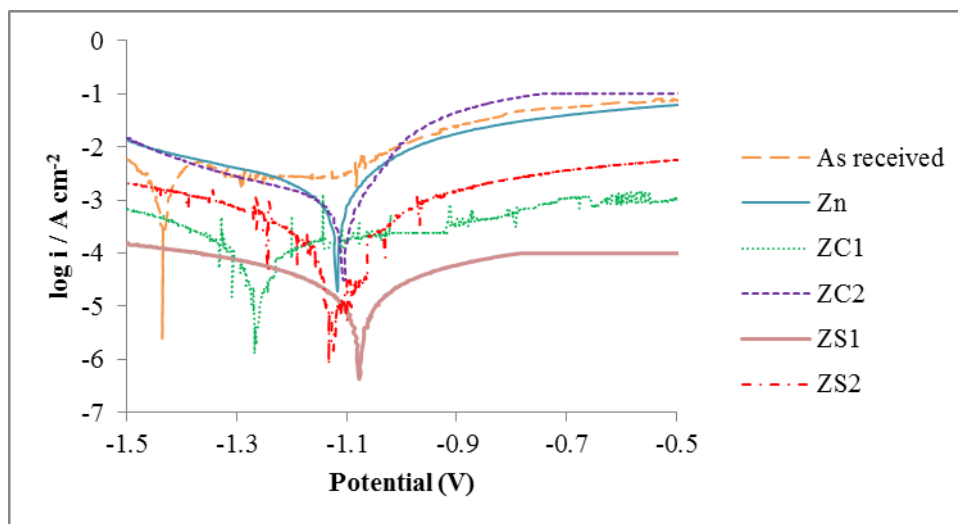


Cathodic process



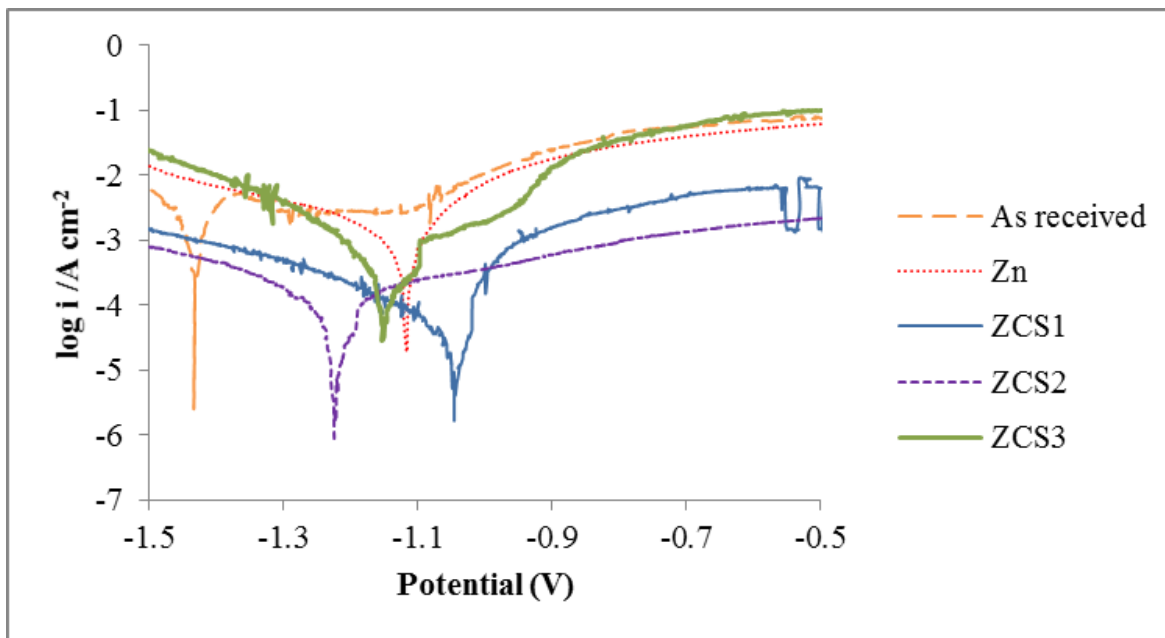
It is evident from the Figure 3 that the potential of the composite based electrodeposits excluding ZC1 shifted more to the positive than the Zn coating. However, a drastic improvement in corrosion potential has been observed for all the coatings in comparison with the as received sample. This result suggests that the composite coatings exhibit better corrosion resistance than as received and Zn coating. Cr<sub>2</sub>O<sub>3</sub> composite samples (ZC) shows a positive shift in potential from -1.2 to -1.11V when the Cr<sub>2</sub>O<sub>3</sub> content in the bath was increased from 10 to 20 g/L. The current density of the matrix was reduced from 12.8 to 10.7  $\mu\text{A}/\text{cm}^2$  due to the addition of 20 g/L Cr<sub>2</sub>O<sub>3</sub> nanoparticles in the plating bath. This result denotes that the increasing particle content of Cr<sub>2</sub>O<sub>3</sub> in the bath has significant influence in the corrosion resistance of Zn based coatings. The composite electrochemical behavior resulted from the increment of Cr<sub>2</sub>O<sub>3</sub> particles comply with Guglielmi 's two step adsorption model. This model suggest that the increased bath particle content promotes the availability of particles to be codeposited on the cathode. However, the improved corrosion resistance shown by ZC2 nanocomposite coating is not in accordance with the results obtained by Srivastava et al. [11]. The author studied the electrochemical influence of nano-Cr<sub>2</sub>O<sub>3</sub> incorporation into Ni matrix and no significant improvement in corrosion resistance was observed at a particle loading of 50g/L [11]. The enhancement in corrosion properties obtained in this work suggest that the optimal particle concentration in the electroplating bath can be obtained at lower bath particle loading for improved corrosion resistance. ZS1 nanocomposite showed the highest potential shift and lowest current density as compared to all the binary composite coatings. Further increase in particle content of SiO<sub>2</sub> in the bath yielded no significant results. Increasing of bath particle loading of Al<sub>2</sub>O<sub>3</sub> from 5 to 10 and 15 g/L have been reported to negatively affect the electrochemical behavior of Zn-Ni matrix. The reduction in

corrosion resistance of the matrix was ascribed to the defects that might be generated due to rapid incorporation or agglomeration of the particles in the bath [3].



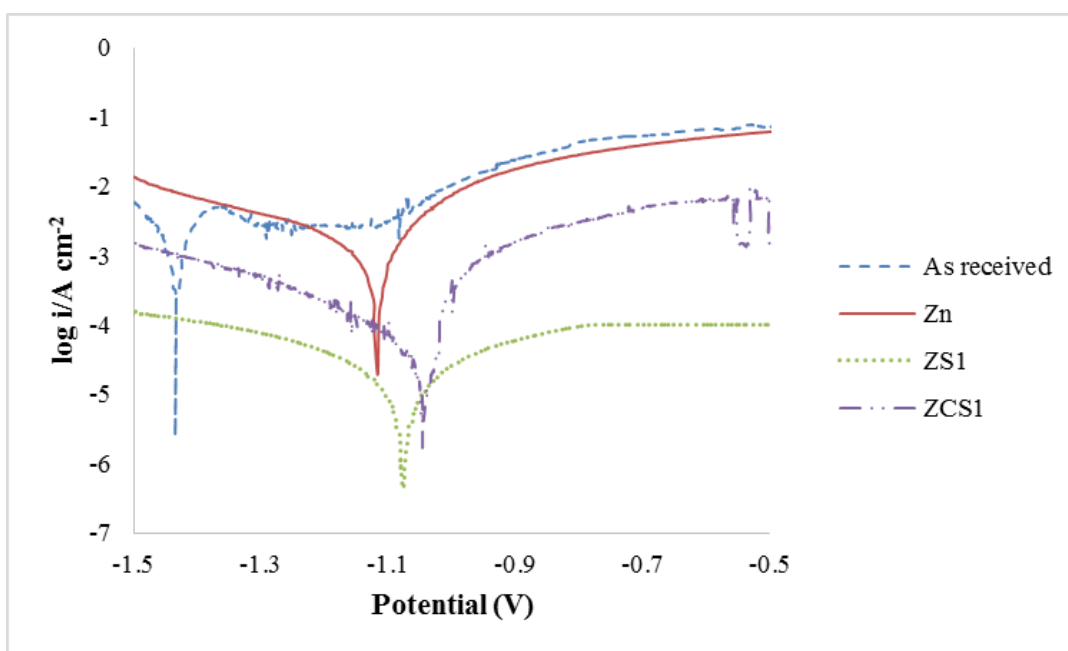
**Figure 3.** Polarization curves of as received, Zn coating, ZC1, ZC2, ZS1 and ZS2 nanocomposite coatings in 3.65% NaCl solution.

Figure 4 shows the electrochemical behavior of the Zn ternary alloy. The figure shows a potential shift towards a nobler direction for ZCS1 nanocomposite coating. The addition of 2.5 and 7.5 g/L of both  $\text{Cr}_2\text{O}_3$  and  $\text{SiO}_2$  nanoparticles into the bath respectively, resulted in potential shift of 0.38 V when compared with as received sample and 0.08 V for Zn coating. A corresponding decrease in current density was also noted as a result of these additions. The results obtained indicate that the incorporation of the mixed oxide composite improves the corrosion resistance of Zn matrix. The uniform dispersion of the nanoparticles promote filling of surface defects such as pores, gaps, microholes, etc. in the matrix and thus reducing active sites for corrosion attack.  $\text{SiO}_2$  and  $\text{Cr}_2\text{O}_3$  nanoparticles have been reported to exhibit inhibitory effect on corrosion of a metal matrix [9, 11]. Inclusion of nanoparticles into a metal matrix create an inert physical barrier that isolates the corrosive medium from the matrix. Therefore, the positive potential shift exhibited by ZCS1 nanocomposite coating can be attributed to the incorporation of the mixed oxide composite. Varying the particle content of  $\text{Cr}_2\text{O}_3$  and  $\text{SiO}_2$  nanoparticles in the bath from 2.5 to 7.5 g/L  $\text{Cr}_2\text{O}_3$  and 7.5 to 2.5 g/L  $\text{SiO}_2$  yielded a negative potential shift as it can be seen in ZCS2 and ZCS3 nanocomposites. This result reveal that the improvement in corrosion resistance exhibited by ZCS1 nanocomposite coating is ascribed to the presence of  $\text{SiO}_2$  nanoparticles.  $\text{SiO}_2$  particles are hydrophilic, they constantly interacts with the electrolyte and thus making their incorporation into a metal matrix hard [3]. Therefore, increment of the particle content of  $\text{Cr}_2\text{O}_3$  particles in the bath inhibit the optimum incorporation of  $\text{SiO}_2$ . The negative potential shift and higher corrosion current densities shown by ZCS2 and ZCS3 nanocomposite coatings suggest that ZCS deposits fabricated under these conditions interact strongly with the cathodic reaction. This behavioural trend is similar to the binary system where the addition of more nanoparticles had no positive effect on the corrosion resistance of the coatings.



**Figure 4.** Polarization curves of as received, Zn coating, ZCS1, ZCS2 and ZCS3 nanocomposite coatings in 3.65% NaCl solution.

The comparative plots of the binary and ternary composites are shown in figure 5. ZCS1 nanocomposite coating possesses the highest potential as compared to all other samples. This proves that Cr<sub>2</sub>O<sub>3</sub> and SiO<sub>2</sub> nanoparticles have good synergetic effect of the corrosion resistance of Zn matrix and uncoated mild steel sample (as received).



**Figure 5.** Polarization curves of as received, Zn coating, ZS1 and ZCS1 nanocomposite coatings in 3.65% NaCl solution.

**Table 2.** Corrosion Parameters

Sample	$E_{corr}$ (V)	$I_{corr}$ ( $\mu A/cm^2$ )	$\beta_a$ (V/dec)	$\beta_c$ (V/dec)	CR (mm/yr)
As Received	-1.4329	156.5	0.0208	0.1450	1.3
Zn	-1.1282	12.8	0.0412	0.0901	0.0168
ZC1	-1.2665	37.9	0.1489	0.1036	0.0315
ZC2	-1.1075	10.7	0.0796	0.0511	0.0069
ZS1	-1.0776	8.72	0.0237	0.0466	0.0057
ZS2	-1.1319	48.4	0.1508	0.1367	0.0403
ZCS1	-1.0466	2.44	0.0214	0.0165	0.0020
ZCS2	-1.2109	44.2	0.1638	0.0346	0.0586
ZCS3	-1.1548	19.3	0.0802	0.0452	0.0178

3.4 Structural analysis

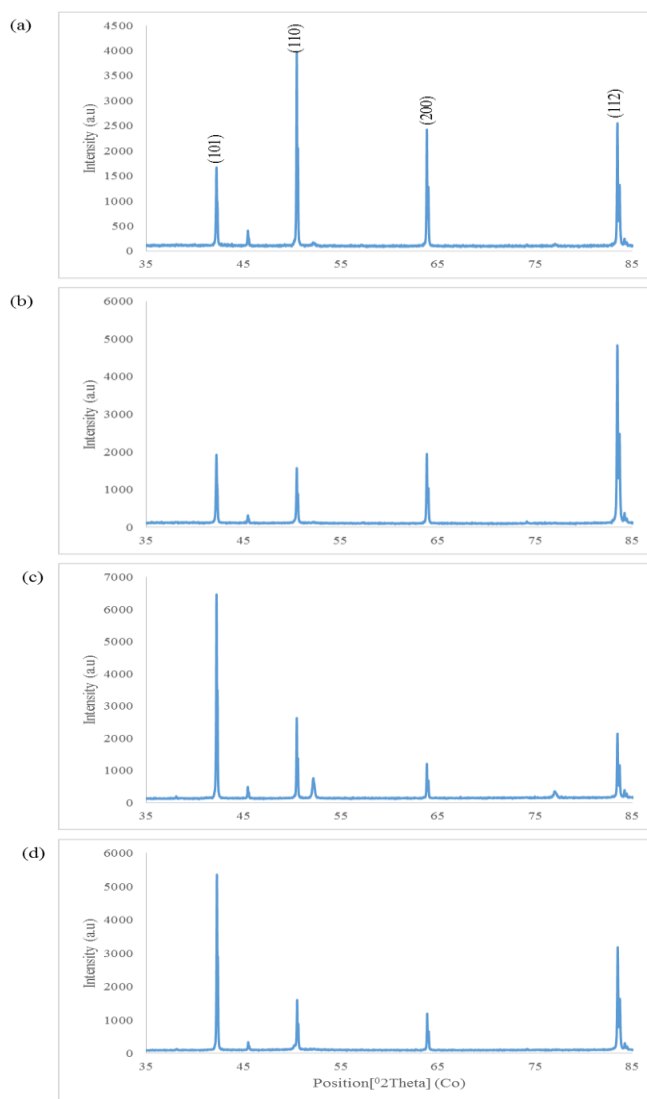


**Figure 6.** XRD diffractograms of plain Zn coating, ZC2, ZS1 and ZCS1 nanocomposite coatings.

XRD diffractograms of plain Zn coating, ZC2, ZS1 and ZCS1 nanocomposite coatings are shown in Figure 6. The majority of the diffraction lines of the diffractograms can be ascribed to the Zn hexagonal structure. The incorporation of the nanoparticles had no effect on the preferential crystallographic orientation of the metal matrix and follows a similar pattern as of that displayed by Zn. However, substantial modification of the preferential crystallographic orientation of the metal matrix have been observed for the composite coatings.

Fe (200) and ZnO (110) peaks have also been identified and they are drastically reduced by the incorporation of the nanoparticles. The reduction of the Fe peak shows that the nanoparticles promotes a formation of a deposit that better cover the surface of mild steel. The Fe peak of ZCS1 composite coating (figure 6d) is reduced than that of all the composites indicating good synergetic properties of the mixed-oxide nanocomposite. The slight peak broadening of the composites suggest that the nanoparticles retard grain growth and creates more nucleation sites resulting in uniform and small sized grains [2].

### 3.5 Surface Morphology

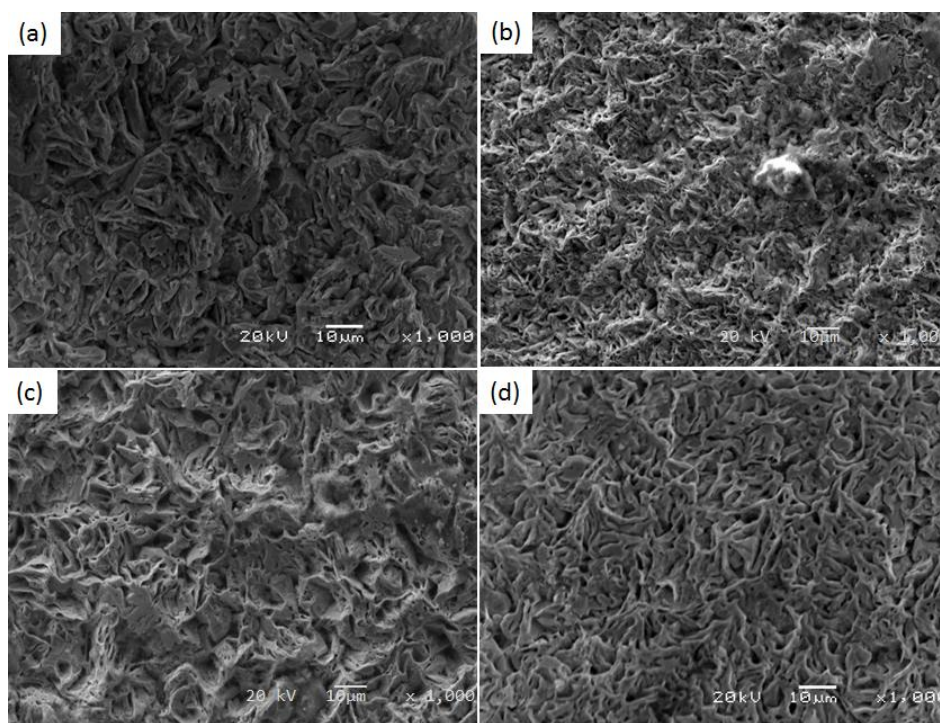


**Figure 7.** SEM micrographs for the coatings (a) Zn coating, (b) ZC2, (c) ZS1 and (d) ZCS1 nanocomposite coatings.

SEM images of zinc and zinc composite electrodeposits are shown in figure 7. An appreciable microstructural orientation modification can be observed in the composite coatings compared with the zinc sample. The surface morphology of zinc shows a flake-like crystal structure as presented by figure 7 (a). All the composite based samples show almost a similar crystal structure but ZC2 and ZCS1 display a more dendritic grain arrangement. The arrangement of the grains exhibited by the composites

are more compact and contain finer grains than the Zn coating which shows gaps, microholes and pores. The surface modification can be attributed to the incorporation of  $\text{Cr}_2\text{O}_3$  and  $\text{SiO}_2$  nanoparticles which filled up the gaps and the microholes in the metal matrix. ZCS1 (Figure 7d) possessed a more refined microstructure with homogenous nanoparticles dispersion in the Zn matrix compared to all the coatings. The homogeneity in particles dispersion can be ascribed to the uniform distribution of the nanoparticulates in the electroplating bath due by magnetic stirring.

EDS confirmed the presence of the  $\text{Cr}_2\text{O}_3$  and  $\text{SiO}_2$  particles in the coating as shown in figure 8. This proved that the bi-inclusion of the particles positively influenced the surface orientation of the coatings. ZC2 (figure 7b) follows a similar surface morphological orientation as ZCS1 with homogeneous and uniformly distributed nanoparticles in the matrix. Several authors reported the incorporation of  $\text{SiO}_2$  and  $\text{Cr}_2\text{O}_3$  to inhibit grain growth of metal matrix resulting in small sized grains [9, 11].

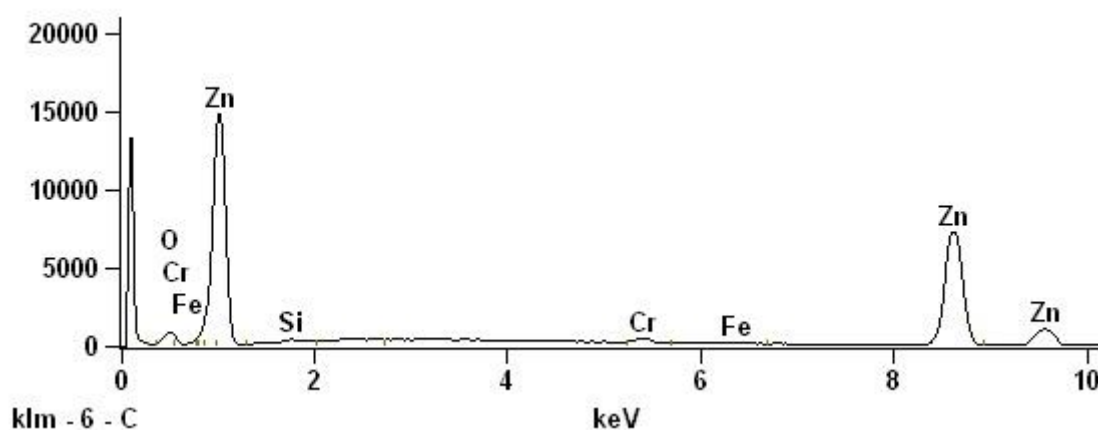


**Figure 8.** EDS spectrum of Zn-7.5g  $\text{Cr}_2\text{O}_3$ -2.5g  $\text{SiO}_2$  (ZCS1) composite alloy coating

### 3.6 Thermal Stability

Figure 9 shows Zn and Zn composites coatings exposed to  $250^\circ\text{C}$  of heat treatment for a time range of 0.5, 2 and 16 hours. After each exposure to annealing temperature, the coatings were tested for microhardness to evaluate the thermal stability of the coatings. The composites exhibited higher microhardness values throughout the tests compared to Zn coatings. The constant higher microhardness values can be attributed to the incorporation of the nano- $\text{Cr}_2\text{O}_3$  and  $\text{SiO}_2$ . However, it can be seen that high reduction in microhardness is evident at time range between 0.5 and 2 hours. This behavior can be ascribed to the rapid grain growth or surface oxidation phenomena as reported by Apachitei et al [18]. For the first 30 minutes, the ternary composite (ZCS1) exhibited the lowest loss in microhardness (4.04%) but the values decreased with the time of exposure of heat treatment. On the other side, the binary composite (ZC2) recorded the highest loss of microhardness (28.2%) in the first 30 minutes of exposure to high temperatures but became stable with time up to 16 hours. This result suggest that  $\text{Cr}_2\text{O}_3$  and  $\text{SiO}_2$  nanoparticles have good synergetic effect on the thermal stability of Zn

based coatings at 250 °C for limited time by inhibiting grain growth. However exposure to prolonged time reduces the ability of the mixed oxide composite to inhibit grain growth and surface oxidation. ZCS1 performed poorly than all the composites after 30 minutes and ZC2 yielded better results than all the samples. The microhardness values of the composite were kept higher than the plain Zn coatings up to 16 hours.

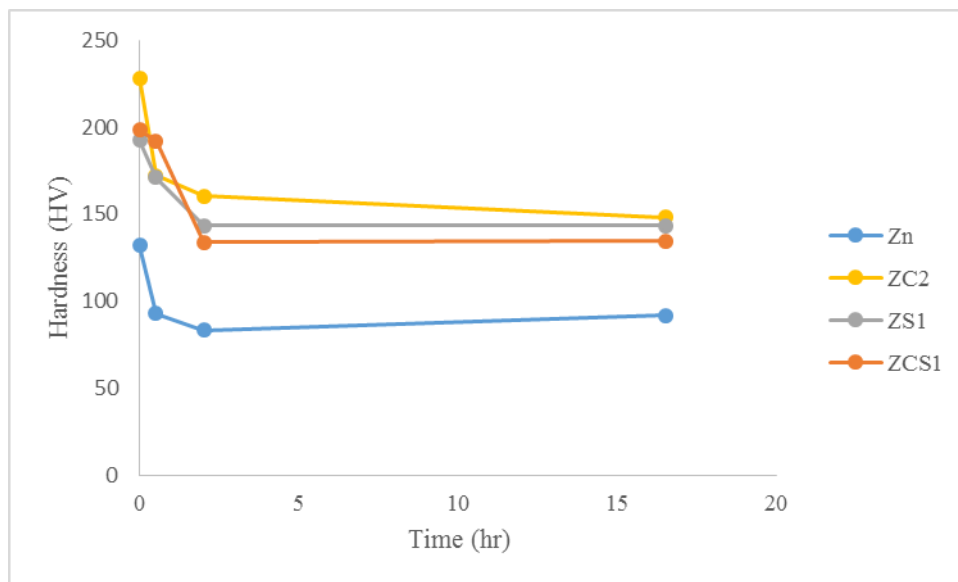


**Figure 9.** Effect of heat treatment on microhardness of zinc coated samples

### 3.7 Tribological behavior

Figure 10 shows coefficient of friction vs time for as received sample, Zn and Zn nanocomposite coatings. All the composite coatings displayed reduced coefficient of friction than as received and Zn coatings throughout the testing time. Table 3 presents the average coefficients of friction of all the samples. Mild steel showed the highest coefficient of friction of 0.13 followed by plain Zn (0.074) and these values were reduced to 0.016 when  $\text{Cr}_2\text{O}_3$  nanoparticles were incorporated into Zn matrix.

Zn- $\text{Cr}_2\text{O}_3$  (ZC2) exhibited the lowest coefficient of friction than all the composites and this include the ternary composite (ZCS1). This result can be attributed to the barrier that is formed by a large fraction of adsorbed on the coating between the metal matrix and the reciprocating tungsten carbide ball. This barrier reduces a direct contact of the metal matrix with the tungsten carbide ball and hence reduced coefficient of friction due to the self-lubrication properties of the nanocomposite particles. The reduced coefficient of friction exhibited by the composites may also suggest that the particles impart lubricating properties to the Zn coatings.

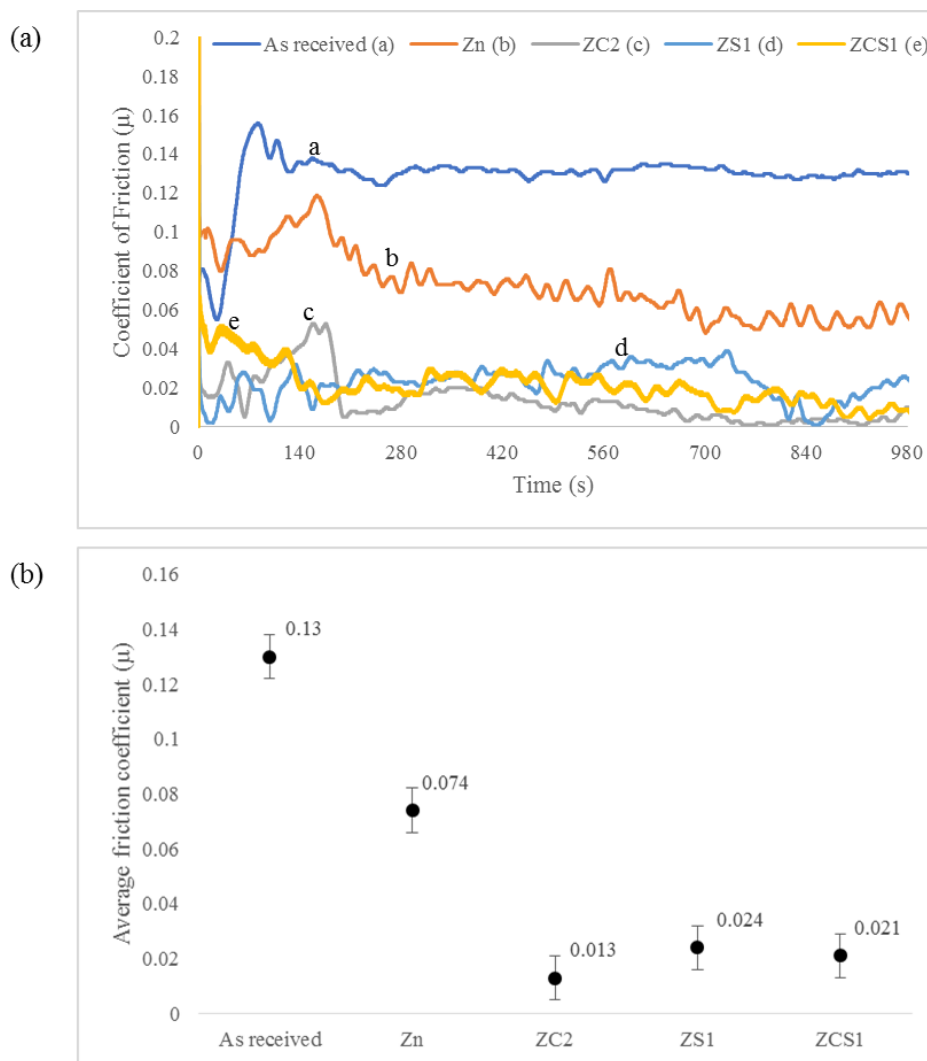


**Figure 10.** Friction coefficient vs time for as received, Zn and Zn-Cr<sub>2</sub>O<sub>3</sub> and SiO<sub>2</sub> nanocomposite coatings

The morphological characteristics of the worn out surfaces obtained from non-lubricated conditions at room temperature are shown in figure 11. Micro-ploughing is evident on the surface of as received (figure 9a) caused by the counter ball. The surface wear deterioration of as received sample occurred as a result of this plastic deformation and led to the formation of micro-cracks and grooves. The type of wear revealed by the behavior of this sample is abrasive. The coatings are categorized by surface peeling of the coating but the degree of damage of Zn (figure 9b) is severe as compared to the composite alloys. Instability of the coating adhesiveness propagated by the wearing action of the counter ball characterized by flaking can be observed in ZC2 and ZS1 (figure 9c and d) but the wear depth is shallower compared to Zn. ZCS1 exhibit minimal flaking of the coating when compared to all the coatings.

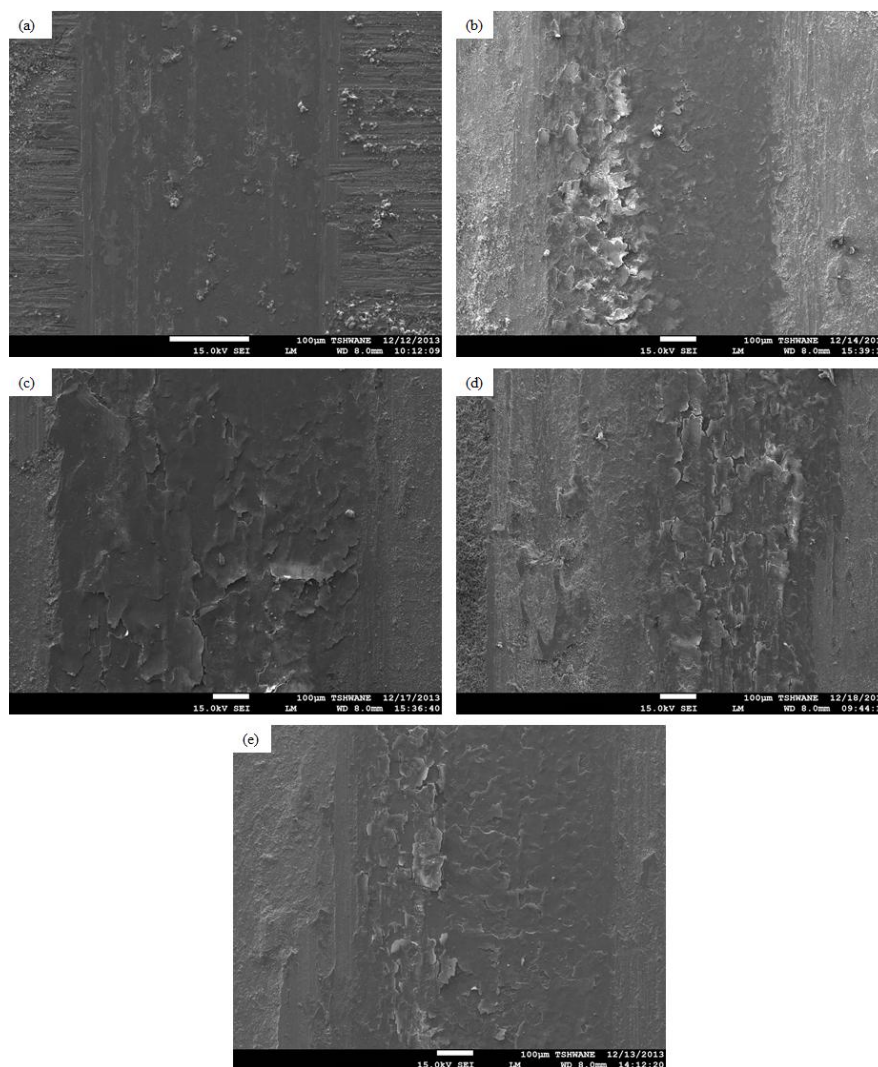


**Figure 11.** SEM micrographs of the worn out surfaces (a) as received (b) Zn coating (c) ZS1 binary nanocomposite coating (d) ZC2 binary nanocomposite coating (e) ZCS1 ternary nanocomposite coating

The wear loss tests were carried out under dry sliding condition using silica sand as the wearing media at a normal load of 5N. Figure 12 shows the percentage wear loss for as received sample, Zn coating, ZC2, ZS1 and ZCS1 nanocomposite deposits. The composite coatings showed reduced mass loss as compared to the as received sample (0.695%) and plain Zn coating (0.517%). This result suggest that the incorporation of the nanoparticles of  $\text{Al}_2\text{O}_3$  and  $\text{Cr}_2\text{O}_3$  into the Zn matrix imparts protective barrier between the matrix and the wearing wheel. Therefore, the inclusion of these nanoparticles have positive significance on the wear resistance of Zn coatings. ZC2 (0.393%) and ZS1 (0.382%) exhibited similar wear loss behavior and no significant change in wear resistance was observed between the two samples. However, when the nanoparticles were incorporated into the Zn matrix as a mixed oxide, a drastic reduction in mass loss (0.176%) was observed. This result proved that incorporation of  $\text{Al}_2\text{O}_3$  and  $\text{Cr}_2\text{O}_3$  nanoparticles as a mixed-oxide composite has positive synergetic effect on the wear resistance of Zn matrix.

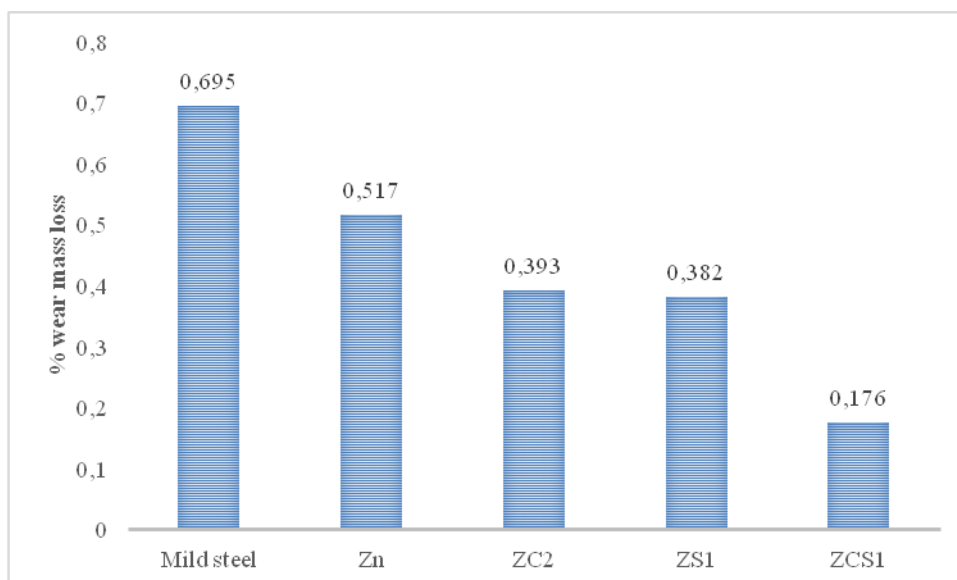


**Figure 12.** Percentage wear mass loss of as received, Zn and Zn nanocomposite coatings obtained under dry sliding conditions at load of 5N and speed of 200 rev/min.

#### 4. CONCLUSIONS

Zn-Cr<sub>2</sub>O<sub>3</sub>-SiO<sub>2</sub> nanocomposite coatings were successfully prepared by electrodeposition technique onto mild steel substrates. The microstructure of the composites revealed flake-like crystalline structure which was similar to the one of Zn but with finely and uniformly distributed grains. This proved that the incorporation of the mixed oxide composite have significant effect on the microstructure of Zn matrix. The ternary composite coating (ZCS1) yielded the highest corrosion resistance more than all the samples. This result showed that Cr<sub>2</sub>O<sub>3</sub> and SiO<sub>2</sub> nanoparticles have good synergetic effect on the corrosion resistance of Zn based coatings. Improvement in microhardness and thermal stability was evident after the evaluation of the coatings for hardness and exposing them to annealing temperatures of 250 °C up to 16 hours. Reduction in coefficient of friction proved the coatings to possess self-lubricating properties and hence improvement in wear resistance. This investigation revealed that the incorporation of the Cr<sub>2</sub>O<sub>3</sub> and SiO<sub>2</sub> into Zn matrix has positive synergetic effect on the microhardness, thermal stability and tribology but not on the corrosion resistance.

#### ACKNOWLEDGEMENT

This material is based upon work supported financially by the National Research Foundation. The equipment support by Surface Engineering Research Centre (SERC) Tshwane University of Technology, Pretoria is deeply appreciated.

#### References

1. W.S. Khan and R. Asmatulu, "Nanotechnology Emerging Trends, Markets, and Concerns. Nanotechnology safety".pp. 1-16, Elsevier, Amsterdam (2013).

2. K. Vathsala and T.V. Venkatesha, *Appl. Surf. Sci.*, 257 (2011) 8929.
3. D. Blejan and L.M. Muresan, *Materials Corr.*, 64 (2013) 433.
4. H. Zheng and M. An, *J. Alloys. Compd.*, 459 (2008) 548.
5. B.M. Praveen and T.V. Venkatesha, *Appl. Surf. Sci.*, 254 (2008) 2418.
6. S. Ranganatha, T.V. Venkatesha, K. Vathsala and M.K. Punith kumar, *Surf. Coat. Technol.*, 208 (2012) 64.
7. J. Fustes, A. Gomes, M.I. da Silva Pereira, *J Solid State Electrochem*, 12 (2008) 1435–1443.
8. O. Sancakoglu, O. Culha, M. Toparli, B. Agaday and E. Celik, *Materials and Design*, 32 (2011) 4054.
9. O. Hammami, L. Dhouibi, P. Bercot, E. Rezrazi, E. Triki, *Int. J. Corr.*, 12 (2011) 1.
10. T. Borkar. Electrodeposition of nickel composite coatings. Master of Science. Oklahoma State University, 45-75 (2010).
11. M. Srivastava, J.N. Balaraju, B. Ravishankar and K.S. Rajam, *Surf. Coat. Technol.*, 205 (2010) 66.
12. C.K. Lee, *Tribology Int*, 55 (2012) 7-14.
13. O.S.I. Fayomi, A.P.I. Popoola and C.A. Loto, *Int. J. Electrochem. Sci.*, 9 (2013) 3885.
14. C.M. Müller, M. Sarret and M. Benballa, *Surf. Coat. Technol.*, 162 (2002) 49.
15. L. Kong, Q. B. S. Zhu, J. Yang and W. Liu, *Tribology Int.*, 45 (2012), 43.
16. C.S. Ramesh and S.K. Seshadri, *Wear*, 255 (2003) 893.
17. N. Guglielmi, *J. Electrochem. Soc.*, 119 (1972) 1009.
18. I. Apachitei, F.D. Tichlaar, J. Duszczuk and L. Katgerman, *Surf. Coat. Technol.*, 149 (2002) 263.
19. S.R. Yu, Y. Liu, W. Li, J.A. Liu and D.S. Yuan, *Composites: Part B.*, 43 (2012) 1070.
20. R.K. Saha and T.I. Khan, *Surf. Coat. Technol.*, 205 (2010) 890–895.
21. K. Kondo, A. Ofgishi and Z. Tanaka, *J. Electrochem. Soc.*, 147 (2000) 2611.
22. T.J. Tuaweri and G.D. Wilcox, *Surf. Coat. Technol.*, 200 (2006) 5921.
23. A. Salah, B. Makhouloufa, H. Zinab, H. Bakra and M.S. Al-Attara, *Materials Sci. Eng. B.*, 178 (2013) 337.